

# *In Vivo* Biodistribution of a Humanized Anti-Lewis Y Monoclonal Antibody (hu3S193) in MCF-7 Xenografted BALB/c Nude Mice

Kerrie Clarke, Fook-Thean Lee, Martin W. Brechbiel, Fiona E. Smyth, Lloyd J. Old, and Andrew M. Scott<sup>1</sup>

Tumour Targeting Program, Ludwig Institute for Cancer Research, Melbourne Branch, Austin and Repatriation Medical Centre, Heidelberg, Victoria 3084, Australia [K. C., F. T. L., F. E. S., A. M. S.]; Radioimmune and Inorganic Chemistry Section, Radiation Oncology Branch, National Cancer Institute, NIH, Bethesda, Maryland 20892-100 [M. W. B.]; Ludwig Institute for Cancer Research, Memorial Sloan Kettering Cancer Center, New York, New York 10021 [L. J. O.].

## ABSTRACT

The biodistribution characteristics of a humanized anti-Lewis<sup>y</sup> antibody (hu3S193) radiolabeled to three radioisotopes, <sup>125</sup>I, <sup>111</sup>In, and <sup>90</sup>Y, were examined in a BALB/c nude mouse xenograft model of breast cancer. The immunoreactivity of both <sup>125</sup>I- and <sup>111</sup>In-bound hu3S193 exceeded 50% and was 20% for <sup>90</sup>Y. *In vivo*, labeled antibody was shown by gamma camera imaging and immunohistochemical and autoradiographic techniques to localize to Lewis<sup>y</sup>-expressing breast xenografts with minimal normal tissue uptake. Maximal radioisotope uptake peaked at 48 h for all three isotopes; however, the percentage of injected dose/gram and tumor retention were greater for <sup>111</sup>In- and <sup>90</sup>Y-bound antibody than for <sup>125</sup>I-bound antibody. Although immunoreactivity of <sup>111</sup>In- and <sup>125</sup>I-labeled hu3S193 in serum was stable over a 5-day period, the amount of unlabeled <sup>111</sup>In in serum was lower than <sup>125</sup>I, which together with higher tumor uptake indicates better retention of <sup>111</sup>In-labeled hu3S193 and catabolites within the tumor cells. Superior tumor uptake and retention of <sup>111</sup>In-labeled hu3S193 and similar blood clearance compared with <sup>125</sup>I-labeled hu3S193, suggest that radiometals are the preferred radioisotope for this antibody-antigen system. Humanized 3S193 is a promising new construct for the targeting and potential therapy of Lewis<sup>y</sup>-expressing tumors.

## INTRODUCTION

Despite advances in the treatment of breast cancer in terms of new chemotherapeutic and hormonal agents, the median survival of patients with advanced breast cancer has remained virtually constant over the last 30 years, and recurrent breast cancer remains incurable (1). New treatment strategies are required if there is to be any impact on the current plateau in survival. Conventional radiotherapy and chemotherapy are delivered to both normal and neoplastic cells, relying upon the enhanced sensitivity of rapidly dividing cancer cells to achieve preferential killing (2). In contrast, mAbs<sup>2</sup> can be directed or “targeted” against tumor associated antigens which may be expressed on the surface of the tumor cells (3).

A number of tumor antigens have been shown to have high expression on malignant breast cancer cells, including HER2/neu, MUC, carcinoembryonic antigen, and Le<sup>y</sup> (3). The Le<sup>y</sup> antigen is a family member of the blood group-related difucosylated oligosaccharides with chemical structure Fuc $\alpha$ 1 $\rightarrow$ 2Gal $\beta$ 1 $\rightarrow$ 4[Fuc $\alpha$ 1 $\rightarrow$ 3] GlcNAc $\beta$ 1 $\rightarrow$ R(4). They are associated with 60–90% of human carcinomas of epithelial cell origin including breast, colon, gastric, and lung cancer (5–7). The high frequency of Le<sup>y</sup>-expressing tumors, high density of Le<sup>y</sup> on tumor cell surface, and relatively homogeneous expression in primary and metastatic lesions have led to its selection as an antigenic target.

3S193 is a mAb produced using standard hybridoma techniques

following immunization of BALB/c nude mice with Le<sup>y</sup>-expressing MCF-7 breast cancer cells. The murine antibody has been shown to have high specificity for Le<sup>y</sup> and reacted strongly in rosetting assays and cytotoxic tests with Le<sup>y</sup>-expressing cells (8). The use of murine mAbs, however, is limited by their immunogenicity. Murine antibodies are recognized as foreign, and the immune system mounts a classical humoral immune response producing HAMAs. Although clinical HAMA requires rechallenge to the same antibody, serum sickness reactions can occur after the first or repeated infusions and are usually unrelated to dose or rate of administration and are manifested principally by myalgias and arthralgias (9). A further limitation of many murine antibodies is their inability to harness the effector and complement response of the human immune system as effectively as humanized antibodies, depending upon the isotype of the antibody (10).

CDR grafting is one method of humanizing antibodies, combining murine antigen binding regions (CDR) with human V-region framework determinants. CDR grafting aims to make the surfaces of the antibody appear as fully human as possible, but retain the murine antigen-binding packaging and interface reactions determining high-affinity binding (11). 3S193 has been humanized by CDR grafting, and the reactivity for Le<sup>y</sup> has been confirmed to be similar to the murine version, and with retained potent effector function of complement-dependent cytotoxicity and antibody-dependent cellular cytotoxicity (8, 12). hu3S193 has only 3–5% murine residues in the antibody variable domain, markedly reducing the potential for an immune response in planned human trials.

The role of conventional radiotherapy in metastatic breast cancer has historically been limited to local palliation. Given that breast cancer is a radiation-sensitive disease (2), targeted delivery of radiation of effective dose to all metastatic sites using mAbs would be a novel and potentially useful therapeutic modality. Radionuclides are attractive agents for selective targeting to tumors by chemical conjugation to antitumor antibodies. The emitted radiation targeted to tumors can be used to kill tumor cells (therapy) or to detect primary or metastatic tumor (imaging), depending on the isotope selected. Considerations in selecting a radioisotope include type of emission, its range, tumor dose rate and total tumor dose, biological half-life, labeling efficiency, and stability. To be effective, the link between the antibody and the radionuclide must be stable *in vivo*, and the labeling procedure must not alter the biodistribution or binding characteristics of the antibody. This study explores such properties of hu3S193 bound to <sup>125</sup>I, <sup>111</sup>In, and <sup>90</sup>Y.

## MATERIALS AND METHODS

**mAbs.** The generation of murine 3S193 using standard hybridoma technique after immunization of BALB/c mice with Le<sup>y</sup>-expressing MCF-7 breast cancer cells and its subsequent humanization has been described previously (8, 12). hu3S193, a CDR grafted version of 3S193, was produced by Scotgen (Aberdeen, Scotland) in conjunction with the Ludwig Institute for Cancer Research. hu3S193 used for the experiments outlined was obtained from both the New York Branch, and the Biological Production Facility of the Melbourne Branch of the Ludwig Institute for Cancer Research. huA33, a humanized

Received 12/9/99; accepted 7/6/00.

The costs of publication of this article were defrayed in part by the payment of page charges. This article must therefore be hereby marked *advertisement* in accordance with 18 U.S.C. Section 1734 solely to indicate this fact.

<sup>1</sup> To whom requests for reprints should be addressed, at Ludwig Institute for Cancer Research, Austin and Repatriation Medical Centre, Heidelberg, Victoria, 3084, Australia. Phone: (613) 9496-5876; Fax: (613) 9496-5892; E-mail: ams@austin.unimelb.edu.au.

<sup>2</sup> The abbreviations used are: mAb, monoclonal antibody; Le<sup>y</sup>, Lewis<sup>y</sup> antigen; HAMA, human anti-mouse antibodies; CDR, complementarity determining region; hu, humanized; ITLC, instant thin layer chromatography; CHX-A<sup>32</sup>-DTPA, C-functionalized *trans*-cyclohexyldiethylenetriaminepentaacetic acid; %ID/g, percent injected dose/gram; IR, immunoreactivity.

antibody directed against a novel antigen found in >95% of colorectal cancers (13), was supplied by the New York Branch of the Ludwig Institute and used as a subclass-specific control.

**Cell Lines.** MCF-7, a  $Le^y$ -expressing human breast adenocarcinoma cell line originally derived from the pleural effusion of a 69-year-old woman with estrogen receptor-positive metastatic breast cancer (14), was obtained from the American Type Culture Collection (Rockville, MD). SW1222, a  $Le^y$ -negative human colonic cancer cell line, was a gift from the tumor cell bank of the New York Branch of the Ludwig Institute and was used as a control cell line.

Cells were grown in 175-cm<sup>2</sup> plastic flasks (Nunc; Nunc, Roskilde, Denmark) and maintained in log-phase growth in RPMI 1640 (Trace Biosciences, Sydney, Australia) supplemented with 10% (MCF-7) or 5% (SW1222) FCS (MultiSer; Trace Biosciences, Sydney, Australia), 100 units/ml penicillin, 100 µg/ml streptomycin, 0.25 ml/l insulin, 2 mM glutamine, and essential amino acids. Cells were cultured at 37°C in a 5% CO<sub>2</sub> incubator (Forma Scientific, Inc., Marietta, Ohio) and passaged with 0.05% EDTA/PBS (BDH Chemicals, Merck, Melbourne, Australia). Cell viability in all experiments, as determined by trypan blue exclusion, exceeded 90%.

**Radiolabeling and Quality Assurance.** hu3S193 and control antibody (huA33) were labeled with three isotopes, <sup>125</sup>I, <sup>111</sup>In, and <sup>90</sup>Y. Isotopes were obtained from DuPont (Life Science Products, Boston, MA). Radioiodination was performed using a modification of a previously published chloramine-T reaction (15) using a 2-fold molar excess of chloramine-T (Merck, Darmstadt, Germany) over antibody, dissolved in 0.5 M potassium phosphate buffer (pH 7). After a brief 2-min incubation period, the reaction was stopped by adding a 5-fold excess of sodium metabisulfite, again dissolved in a 0.5 M phosphate buffer, and then purified through a desalting column (P6DG; Bio-Rad, Sydney, Australia) equilibrated with PBS.

Antibody labeling with <sup>90</sup>Y and <sup>111</sup>In was achieved via a bifunctional metal ion chelating agent, CHX-A'-DTPA (16) using a modification of a method published previously (17). In brief, a dialysis bag with a  $M_r$  cutoff of 10,000 (Novex, Sydney, Australia) was treated with 10 mM sodium bicarbonate and soaked in deionized water and 1 mM EDTA (pH 7.0) to remove heavy metals. hu3S193 was dialyzed against a 50 mM sodium bicarbonate buffer (pH 8.6) containing 0.15 M NaCl for 6 h. CHX-A'-DTPA was added in molar excess of 5:1 and incubated at room temperature overnight in the dark. Excess unbound antibody was removed by 8 h dialysis with 20 mM sodium acetate buffer containing 0.15 M NaCl (pH 6.3). <sup>111</sup>In or <sup>90</sup>Y were bound to CHX-A'-DTPA antibody conjugate under mildly acidic conditions (pH 5.5) for 20 min, and then the pH was raised to 7 by the addition of small aliquots of 2.0 M sodium acetate, followed by 10 mM EDTA. The radiolabeled mixture was purified by centrifugal desalting on a Sephadex G50 column (Pharmacia, Uppsala, Sweden) equilibrated with PBS.

Radiolabeling was performed on the day of injection into mice. Prior to injection, the percentage of unbound radionuclide content was determined by ITLC, and binding ability of the final radiolabeled product was tested by a  $Le^y$ -positive cell binding (Lindmo) assay as detailed below. Scatchard analysis was used to determine the binding constant ( $K_a$ ) and number of antibody molecules bound per cell for <sup>125</sup>I- and <sup>111</sup>In-labeled antibody.

**ITLC.** The amount of free versus bound antibody following radiolabeling was determined by ITLC as described previously (17, 18). Aliquots of radiolabeled hu3S193 were placed on the origin of standard silica gel impregnated glass fiber ITLC strips (Gelman Scientific, Ann Arbor, MI). To determine the percentage of bound <sup>111</sup>In, ITLC strips were developed using 10 mM EDTA (pH 4.5) and 0.9% saline/10 mM NaOH solution as solvents. In EDTA, hu3S193 remains at the origin, and the CHX-A'-DTPA-<sup>111</sup>In or <sup>90</sup>Y, and free <sup>111</sup>In or <sup>90</sup>Y, respectively, migrate with the solvent front. In 10 mM NaOH solution, hu3S193 and free radionuclide remain at the origin, and CHX-A'-DTPA-radionuclide migrates with the solvent front. Strips were developed until the solvent migrated to the end, and then they were cut in half and counted on a gamma camera. Radioactivity in the bottom half of the strip was calculated as a percentage of the entire strip (top plus bottom). The percentage of free radionuclide was determined by subtraction (NaOH - EDTA). Results were performed in duplicate. Ten % trichloroacetic acid was used as the solvent to determine the percentage of unbound <sup>125</sup>I, with free iodine migrating with the solvent front and bound remaining at the origin. The percentage of isotope bound to hu3S193 was >90% in all experiments detailed.

**IR.** IR of radiolabeled hu3S193 to MCF-7 target cells was determined by linear extrapolation to binding at infinite antigen excess using a "Lindmo"

assay (19). Fifteen to 20 ng of radiolabeled hu3S193 were added to a range of MCF-7 cell concentrations and incubated for 45 min at room temperature with continuous mixing throughout to keep the cells in suspension. Cells were washed three times to remove unbound antibody, and pellets were measured in a gamma counter (Cobra II, Model 5002, Auto-gamma; Packard Instruments, Canberra, Australia). Three samples of radiolabeled hu3S193, at the same concentration as that initially added to the cells, were measured at the same time as cell pellets and the percentage of binding of hu3S193 to MCF-7 cells was calculated by the formula: (cpm cell pellet/mean cpm radioactive antibody standards) × 100. The percentage of binding was graphed against MCF-7 cell concentration using Sigmaplot for Windows (Jandel Scientific, San Rafael, CA), and IR was calculated as the Y-intercept of the inverse plot of both values. Cell pellets to which >100-fold unlabeled hu3S193 was added, prior to radiolabeled hu3S193, were used as a control to determine background cpm.

Scatchard analysis was used to calculate the apparent association constant ( $K_a$ ) and number of antibody molecules bound per cell (19). Unlabeled hu3S193 at concentrations ranging from 5 to 200 µg/ml were added to  $12 \times 10^6$ /ml MCF-7 cells and mixed, and subsequently 30 ng of labeled hu3S193 were added. After 45 min incubation, the cells were washed and counted as described above for Lindmo assay. The IR fraction was taken into account in calculating the amount of free, reactive antibody [(100 - % bound)/100 × total antibody × IR fraction], and specific binding (nm; total antibody × % bound) was graphed against specific binding/reactive free. The association constant was determined from the negative slope of the line. The number of hu3S193 molecules bound per cell was derived by: [(X-intercept of Scatchard plot (nm)/1000) × (6.023 × 10<sup>23</sup>)]/number of cells used in the assay ( $12 \times 10^6$ ).

**Animal Model.** *In vivo* tissue biodistribution studies were performed in female athymic BALB/c nude mice, 5–6 weeks of age, homozygous for the *nu/nu* allele, bred by the SPF Facility, University of South Australia (Adelaide, Australia). Mice were maintained in autoclaved microisolator cages housed in a positive pressure containment rack (Thoren Caging Systems, Inc., Hazelton, PA).

To establish MCF-7 human breast xenografts, mice were supplemented with exogenous estrogen (20, 21). After light Ethrane anesthesia, a 60-day slow release estrogen pellet (0.72 mg estradiol/pellet; Innovative Research of America, Sarasota, FL) was inserted using aseptic techniques into a small s.c. pocket fashioned between the shoulder blades. The surgical incision was closed with a single stitch (6-0 absorbable Dacron or silk). MCF-7 cells ( $25 \times 10^6$ ) in 100–150 µl of medium were subsequently injected s.c. into the left inguinal mammary line. SW1222, non- $Le^y$ -expressing, colon cancer xenografts were established by injection of  $10 \times 10^6$  cells in the right inguinal area of each mouse as a control tumor. The growth rates of both tumors differed. To obtain comparable tumor sizes, the more rapidly growing SW1222 colon cancer cells were injected 4 weeks after inoculation of MCF-7 tumors. Both tumors were of a size appropriate for use 14 days after this time.

Tumor volume was calculated by the formula [(length × width<sup>2</sup>)/2] (21, 22), where length was the longest axis and width the measurement at right angles to the length.

**Biodistribution Studies.** Two biodistribution studies were performed. In the first study, 41 mice were injected i.v. via the retro-orbital plexus with hu3S193 labeled with 5 µCi of both <sup>125</sup>I and <sup>111</sup>In CHX-A'-DTPA-hu3S193 (total, 10 µg of antibody and 10 µCi of radioactivity) suspended in 150 µl of sterile media. Groups of four to five mice, with a mean (± SD) tumor volume of 647 mg ± 252, were sacrificed by cervical dislocation after light ethrane anesthetic at 4, 24, 48, 72, 96, 120, 168, 240, and 360 h after injection of radiolabeled antibody. Mice were bled via cardiac puncture, and blood was collected into heparinized tubes. Tumors and organs [skin, liver, spleen, intestine, stomach, kidneys, brain, bone (femur), lungs, and heart] were immediately removed, blotted dry, and weighed (Sartorius Basic Balance, Ratingen Germany). All samples were counted in a dual chamber gamma scintillation counter (Cobra II, Auto-gamma; Packard Instruments) using a dual tracer program with standard windows set for each isotope, 15–75 Kev for <sup>125</sup>I and 140–430 Kev for <sup>111</sup>In. Standards prepared from the injected material were counted each time, with tissues and tumors enabling calculations to be corrected for the physical decay of the isotopes. Results of labeled antibody distribution over time were expressed as the % ID/g [(cpm tissue sample/cpm cpm standard) × 100/weight in grams] and as tumor:blood ratios.

A second biodistribution study was also performed to assess the distribution

and localization of  $^{90}\text{Y}$ -labeled antibody. Twenty  $\mu\text{Ci}$  of  $^{90}\text{Y}$ -CHX-A"-DTPA-hu3S193 were injected into the retro-orbital plexus of 25 mice bearing MCF-7 xenografts. One to four mice were sacrificed at time points 4, 24, 48, 72, 120, 168, 240, 336, 408, and 504 h after injection and blood and tumors removed. At the 72-h time point, spleen, bone, liver, and kidney were also excised. % ID/g was calculated as described above.

**Statistical Analysis.** Paired Student *t* tests were performed on the different isotope biodistribution time points in each study and individual organ uptakes to assess any differences observed for statistical significance.

**Pharmacokinetics.** Pharmacokinetics were determined for  $^{125}\text{I}$  and  $^{111}\text{In}$  radioconjugates using a curve-fitting program (SAAM II; University of Washington, Seattle, WA) and assuming a two-compartmental model.

**In Vivo Antibody Stability.** The stability of the iodine and indium label *in vivo* was assessed by the amount of free radionuclide present over time, as determined by ITLC. Blood collected from mice at each time point into heparinized tubes was pooled and spun at  $1000 \times g$  for 15 min to obtain plasma. Two  $\mu\text{l}$  of each sample were spotted onto the origin of two standard ITLC strips. Strips were developed, and the percentage of free indium and iodine was calculated as described previously.

A single point immunoreactivity assay was also performed on each pooled plasma sample to determine the *in vivo* stability of the antibody in terms of binding ability. An aliquot of plasma, volume adjusted to standardize for % ID/g, was added to  $12 \times 10^6$  MCF-7 cells and incubated for 45 min at room temperature. Excess unbound antibody was removed at the end of the incubation period by washing twice with medium, and radioactivity in the washed pellet was measured with a gamma counter. An equal volume of blood as that added to the assay was kept as a standard, and binding of blood to cells was calculated as a percentage of antibody present in the standard.

**Imaging.** To enable qualitative comparison of radiolabeled-antibody localization over time, a single mouse from the  $^{125}\text{I}/^{111}\text{In}$  co-labeled antibody study was anesthetized on four separate occasions. At time points 4, 24, 72, and 120 h, the animal received i.p. injections of 0.2 ml of solution containing 18.7 mg/ml tribromoethanol dissolved in 12.5  $\mu\text{l}$  of isopentyl alcohol and 1 ml of sterile water for injection. Images were obtained using a dual head gamma camera ("Biad"; Trionix Research Laboratories, Twinsbury, OH) linked to a Unix computer system with photopeaks set at 173 KeV and 247 KeV with 20% windows. A medium energy collimator was used to acquire images attributable predominantly to  $^{111}\text{In}$ , with negligible contribution from  $^{125}\text{I}$ . Ten-min images were obtained at each time point. Images were acquired in a  $256 \times 256$ -bit matrix, and a standard of known activity was included in the field of view.

**Autoradiography.** Immediately after sacrifice, an MCF-7 tumor from one mouse at time points 24, 48, 72, and 120 h in the  $^{125}\text{I}/^{111}\text{In}$  biodistribution study was excised, frozen, and sectioned on a cryomicrotome (Zeiss Microm HM 5000, Melbourne, Australia). Sequential 5- $\mu\text{m}$  sections were used for direct autoradiography and for H&E staining. Tissue sections were placed on silane-coated glass slides and allowed to dry. Glass slides were placed face down in contact with emulsion of Hyperfilm-MP film (Amersham Life Science, Little Chalfont, United Kingdom) or standard radiography film. The glass slides and film were enclosed in a cassette and stored at  $-70^\circ\text{C}$ . An image intensifier (Hyperscreen; Amersham) was used for Hyperfilm samples and was located directly behind and in contact with the film (23). Slides and

film were taken up at varying time intervals, and film was developed in a standard automatic film processor. It was not possible to distinguish between  $^{125}\text{I}$  and  $^{111}\text{In}$  using the method described.

**Immunohistochemistry.** Immunohistochemistry was performed to confirm the presence and distribution of Le<sup>y</sup> antigen in tumor xenografts and to examine normal murine tissues for Le<sup>y</sup> antigen expression. Xenografts and normal kidney, liver, lung, spleen, stomach, duodenum, jejunum, ileum, and large bowel were surgically removed, embedded in Tissue-Tek OCT Compound (Diagnostic Division, Elkhart, IN), and cut at 5- $\mu\text{m}$  thickness with a cryomicrotome. Sections were fixed with acetone at  $4^\circ\text{C}$  for 10 min, and nonspecific binding was blocked using a commercial protein blocking agent (Lipshaw Immunon, Pittsburgh, PA). Five  $\mu\text{g}$  of hu3S193 diluted in 1% BSA-PBS were applied to sections and incubated at room temperature for 1 h (primary antibody), rinsed with PBS, and then the secondary antibody (biotinylated IgG1 goat antihuman 1:300; Sigma Immunochemicals) was applied for 30 min. After 10 min immersion in 0.3% peroxidase, streptavidin peroxidase (1:1000) was applied for 30 min, and finally the chromagen 3-amino-9 ethyl carbazole (Sigma Chemical Co., St. Louis, MO) for 20 min was used to develop pink coloration to antigen-positive cells. An isotype-matched huIgG1 control antibody (huA33) and no primary antibody controls were used for each tissue or time point analyzed.

## RESULTS

**Antibody Labeling.** ITLC of radiolabeled antibody prior to injection confirmed 94.5% bound  $^{125}\text{I}$  (6.5% free) and >95.5% bound  $^{111}\text{In}$ -CHX-A"-DTPA. The immunoreactivity of  $^{125}\text{I}$  was 51.5% and for  $^{111}\text{In}$ , 65%.  $K_a$  values for  $^{125}\text{I}$  and  $^{111}\text{In}$  were  $0.71 \times 10^{-7} \text{ M}^{-1}$  and  $1.017 \times 10^{-7} \text{ M}^{-1}$ , respectively, both within the range expected for a carbohydrate antibody (24). The number of antibody molecules bound per cell for each isotope was  $7 \times 10^6$  for  $^{125}\text{I}$  and  $4.62 \times 10^6$  for  $^{111}\text{In}$ . In the  $^{90}\text{Y}$ -CHX-A"-DTPA study, 94.1% of radionuclide was bound to hu3S193; however, immunoreactivity was low at 20%. Scatchard analysis was not performed for  $^{90}\text{Y}$ -labeled antibody.

**Biodistribution.**  $^{125}\text{I}/^{111}\text{In}$ -labeled biodistribution study results are presented in Table 1. The comparison of %ID/gram of  $^{125}\text{I}$ - and  $^{111}\text{In}$ -labeled hu3S193 in MCF-7 and control tumors, blood, and group size at each time point are detailed. The %ID/g of both isotopes in MCF-7 xenografts peaked at 48 h after antibody injection, with the uptake of  $^{111}\text{In}$ -labeled hu3S193 being 3-fold greater than  $^{125}\text{I}$  (30.1% versus 10%, respectively) and reaching statistical significance ( $P = < 0.001$ ). Uptake of hu3S193 within breast tumors was superior for the  $^{111}\text{In}$  label at all time points studied, and of note  $^{111}\text{In}$  uptake was >3-fold that of  $^{125}\text{I}$  at  $t = 48$  h to 360 h inclusive (Fig. 1). The blood levels of both isotopes closely approximated each other throughout the study, declining progressively over time. The tumor:blood ratio for  $^{111}\text{In}$ -labeled hu3S193 peaked at  $5.15 \pm 1.65$  at 168 h, compared with  $2.83 \pm 1.2$  at 120 h for  $^{125}\text{I}$ .

Table 1 Biodistribution of  $^{125}\text{I}$  and  $^{111}\text{In}$  CHX-A"-DTPA labeled hu3S193 in xenografted BALB/c nude mice<sup>a</sup>

Time <sup>b</sup> (h)	<i>n</i> <sup>c</sup>	%ID/g <sup>d</sup> in MCF-7 tumor (mean $\pm$ SD)		%ID/g in blood (mean $\pm$ SD)		%ID/g in SW1222 tumor (mean $\pm$ SD)	
		$^{111}\text{In}$	$^{125}\text{I}$	$^{111}\text{In}$	$^{125}\text{I}$	$^{111}\text{In}$	$^{125}\text{I}$
4	4	6.4 $\pm$ 1.5	5.5 $\pm$ 0.9	25 $\pm$ 2.9	24.7 $\pm$ 2.6	8.7 $\pm$ 1.9	8 $\pm$ 1.6
24	5	24.4 $\pm$ 3.4	9.6 $\pm$ 2	15.1 $\pm$ 1.4	15.2 $\pm$ 1.4	9.2 $\pm$ 0.8	6.7 $\pm$ 0.5
48	5	30.1 $\pm$ 4	10 $\pm$ 3.9	12.2 $\pm$ 1.3	12.4 $\pm$ 1.0	7.9 $\pm$ 1.2	4.7 $\pm$ 0.7
72	5	23.4 $\pm$ 4.8	6.3 $\pm$ 0.9	7.6 $\pm$ 1.8	7.7 $\pm$ 1.8	6.4 $\pm$ 1.1	3.6 $\pm$ 0.8
96	4	24.1 $\pm$ 1.3	6.3 $\pm$ 1.7	6.0 $\pm$ 1.9	6.3 $\pm$ 2.1	7.5 $\pm$ 1.7	3.4 $\pm$ 0.7
120	4	22.6 $\pm$ 5	5.5 $\pm$ 2.4	4.4 $\pm$ 0.6	1.9 $\pm$ 0.3	6.2 $\pm$ 2.0	2.9 $\pm$ 0.6
168	4	17.3 $\pm$ 4.4	4.4 $\pm$ 1.6	3.4 $\pm$ 0.6	3.8 $\pm$ 0.7	3.6 $\pm$ 1.1	1.5 $\pm$ 0.6
240	4	9.5 $\pm$ 1.1	2.3 $\pm$ 0.2	1.9 $\pm$ 0.1	2.0 $\pm$ 0.7	1.8 $\pm$ 0.5	1.0 $\pm$ 0.5
360	4	3.5 $\pm$ 1.2	0.8 $\pm$ 0.3	1.1 $\pm$ 0.5	0.9 $\pm$ 0.5	1.4 $\pm$ 0.6	0.6 $\pm$ 0.3

<sup>a</sup> Mice bearing MCF-7 Le<sup>y</sup> positive and control SW12222 tumors received retro-orbital injections containing 5  $\mu\text{Ci}$  of both  $^{125}\text{I}$ - and  $^{111}\text{In}$ -CHX-A"-DTPA-hu3S193 (total, 10  $\mu\text{g}$  antibody; 10  $\mu\text{Ci}$ ) on day 0. Groups of four to five mice were sacrificed at the indicated times. The blood was collected, and tumors removed, blotted dry and weighed. Radioactivity was measured.

<sup>b</sup> Time in hours after injection of antibody.

<sup>c</sup> Number of mice per time point.

<sup>d</sup> %ID/g was calculated. Data are presented as mean  $\pm$  SD.

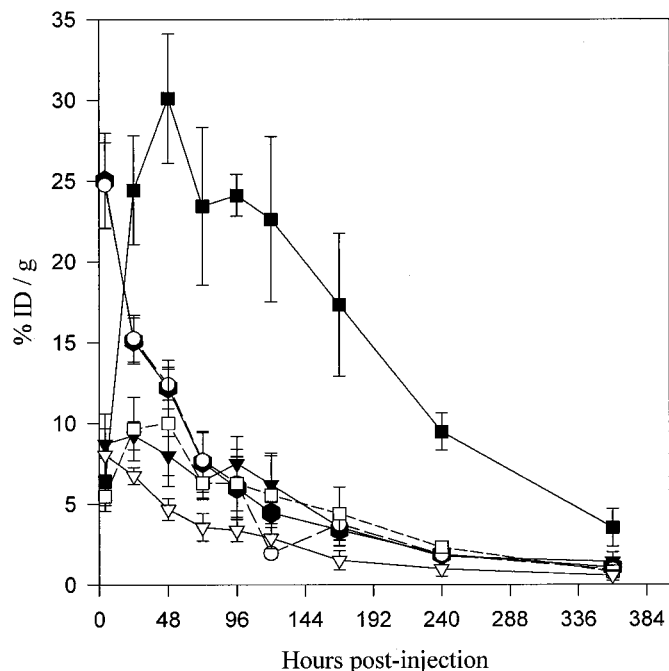


Fig. 1. The biodistribution, expressed as % ID/g over time, of  $^{111}\text{In}$ -CHX-A $^{\alpha}$ -DTPA (closed symbols) and  $^{125}\text{I}$  (open symbols)-labeled hu3S193 in MCF-7 and control (SW1222) tumor xenografts and blood from BALB/c nude mice. Forty-one mice received i.v. injections of a total of  $10\ \mu\text{g}$  ( $10\ \mu\text{Ci}$ ) of radiolabeled hu3S193. Means for each time point, consisting of data from four to five mice, are shown; bars, SD. The data are presented as:  $^{111}\text{In}$ -blood ( $\bullet$ );  $^{111}\text{In}$ -MCF-7 tumor ( $\blacksquare$ );  $^{111}\text{In}$ -control tumor ( $\blacktriangledown$ );  $^{125}\text{I}$ -blood ( $\circ$ );  $^{125}\text{I}$ -MCF-7 tumor ( $\square$ ); and  $^{125}\text{I}$ -control tumor ( $\triangledown$ ).

The biodistribution of radiolabeled hu3S193 in normal murine tissues was studied, and results at 48 and 72 h after injection of radiolabeled hu3S193 are presented in Fig. 2. The % ID/g in all normal tissues was  $<10\%$ . Immunohistochemical analysis demonstrated Le $^y$  expression only in the gastric glands of the stomach and intestinal glands of the jejunum and ileum; this result was consistent with the low uptake of hu3S193 in normal tissues. The uptake of  $^{111}\text{In}$  was only significantly higher than  $^{125}\text{I}$  in the kidney ( $P$ s between  $<0.001$  and  $0.006$ , depending on the time point studied).

Antibody uptake (%ID/g) in SW1222 control tumors was less than that seen in antigen-positive MCF-7 tumors at all time points except 4 h. The higher % ID/g at 4 h in control tumors most likely reflects differences in tumor vascularity between MCF-7 and SW1222 xenografts, with increased vascularity observed in the control SW1222 tumors. Both  $^{111}\text{In}$  and  $^{125}\text{I}$  uptake in control tumors reflected blood pool activity rather than specific tumor uptake, declining progressively over time with no evidence of antibody accumulation within SW1222 tumor xenografts (Figs. 1 and 4).

Results of the  $^{90}\text{Y}$ -hu3S193 study are presented in Table 2, and a comparison to the  $^{111}\text{In}$ -hu3S193 biodistribution study is shown in Fig. 3.  $^{90}\text{Y}$ -labeled antibody uptake in MCF-7 tumors peaked at 22% ID/g ( $t = 48$ –72 h), which was slightly lower but not statistically significantly different ( $P = 0.087$ ) from peak  $^{111}\text{In}$  tumor uptake. At the last time point at which a comparison was made between the two isotopes ( $t = 360$  h), the %ID/g within MCF-7 tumors was 4-fold higher for mice that received the  $^{90}\text{Y}$  label, suggesting prolonged retention of  $^{90}\text{Y}$  within the tumor. Blood clearance for both isotopes approximated each other. At 72 h, hematopoietic organs and kidneys were removed from four mice. Comparison with the results obtained from the  $^{125}\text{I}/^{111}\text{In}$  biodistribution study at the same time points after antibody injection showed higher uptake of  $^{90}\text{Y}$  in kidney, spleen, and bone marrow (%ID/g 9.6, 6.02, and 1.99, respectively). Differences were statistically significant in the kidney compared with  $^{125}\text{I}$  and

$^{111}\text{In}$  ( $P = 0.001$  and  $0.038$ , respectively) and in the spleen compared with  $^{111}\text{In}$  ( $P = 0.009$ ). Differences in bone marrow uptake between the three isotopes were not statistically significant.

**Pharmacokinetics.** The half-life of each isotope bound to hu3S193 was estimated from the %ID/g of blood obtained over the time points sampled. Assuming a two-compartmental model with a four-parameter fit, the mean  $T_{1/2\ \alpha}$  for  $^{125}\text{I}$ -,  $^{111}\text{In}$ - and  $^{90}\text{Y}$ -labeled

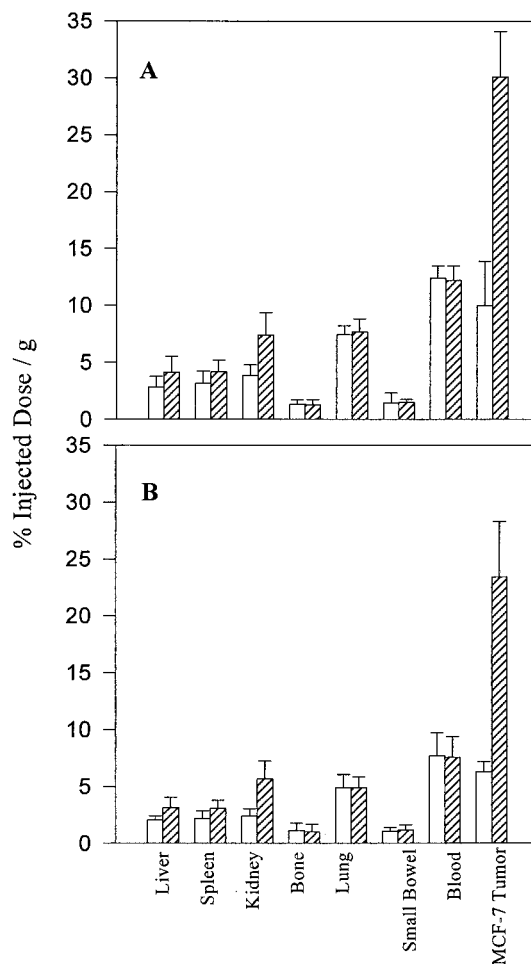


Fig. 2. Biodistribution of  $^{125}\text{I}$ - ( $\square$ ) and  $^{111}\text{In}$ -CHX-A $^{\alpha}$ -DTPA ( $\text{hatched}$ )-labeled hu3S193 in normal murine tissues, MCF-7 tumors, and blood at 48 h (A) and 72 h (B) after injection of BALB/c nude mice. Data from groups of five mice are expressed as mean %ID/g; bars, SD.

Table 2 Biodistribution of  $^{90}\text{Y}$  CHX-A $^{\alpha}$ -DTPA labeled hu-3S193 in MCF-7 xenografted BALB/c nude mice $^a$

Time (h) $^b$	$n^c$	%ID/g $^d$ in MCF-7 tumor (mean $\pm$ SD)	%ID/g in blood (mean $\pm$ SD)
4	3	8.92 $\pm$ 0.93	30.45 $\pm$ 2.48
24	3	13.26 $\pm$ 1.05	14.46 $\pm$ 2.88
48	3	22.47 $\pm$ 4.95	8.54 $\pm$ 2.47
72	4	22.38 $\pm$ 1.87	7.84 $\pm$ 2.15
120	2	18.52 $\pm$ 4.4	5.36 $\pm$ 0.87
168	2	18.96 $\pm$ 5.93	3.0 $\pm$ 1.49
240	4	12.7 $\pm$ 2.2	1.4 $\pm$ 0.95
336	2	8.58 $\pm$ 2.13	1.45 $\pm$ 1.37
408	1	10.3	0.67
504	1	9.62	0.54

$^a$  Twenty  $\mu\text{Ci}$   $^{90}\text{Y}$ -CHX-A $^{\alpha}$ -DTPA-hu3S193 was injected into the retro-orbital plexus of 25 mice bearing MCF-7 xenografts. One to four mice were sacrificed at the indicated times.

$^b$  Time points after injection of antibody. Blood and tumors were removed, blotted dry, and weighed.

$^c$  Number of mice per time point. Radioactivity was measured.

$^d$  %ID/g was calculated. Data are presented as mean  $\pm$  SD.

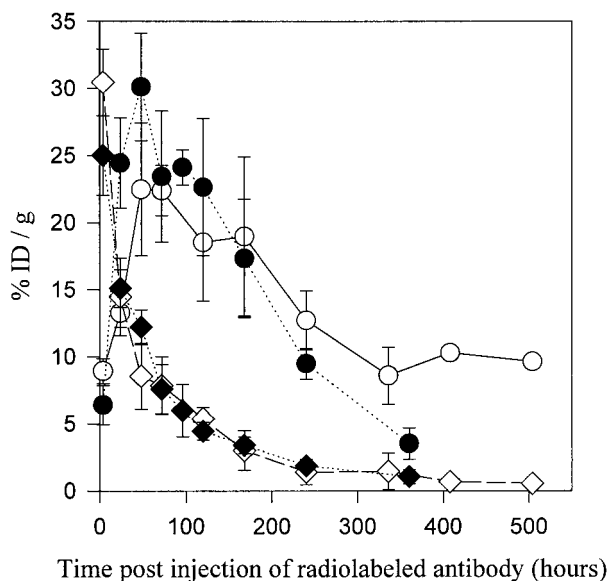


Fig. 3. The biodistribution, expressed as % ID/g, of  $^{90}\text{Y}$ -hu3S193 in blood ( $\diamond$ ) and MCF-7 xenografts ( $\circ$ ) and  $^{111}\text{In}$ -hu3S193 in blood ( $\blacklozenge$ ) and MCF-7 xenografts ( $\bullet$ ) from BALB/c nude mice. Results represent a comparison of two separate biodistribution studies with the individual radiolabels. Groups of one to four mice were sacrificed at time points 4, 24, 48, 72, 120, 168, 240, 336, 408, and 504 h after injection, and blood and tumors were removed. %ID/g was calculated. Data are expressed as means; bars, SD.

3S193 was 9.3, 7.4, and 7.5 h and mean  $T_{1/2}$   $\beta$  69.3, 69.3, and 79 h, respectively.

**In Vivo Stability.** *In vivo* stability was analyzed in the  $^{125}\text{I}$ -hu3S193 and  $^{111}\text{In}$ -hu3S193 study. The percentage of bound  $^{111}\text{In}$ , as determined by ITLC, was  $>99.5\%$  for all time points up to 7 days at which time 98% bound  $^{111}\text{In}$  was present. The percentage of bound  $^{125}\text{I}$  was lower at baseline (93.5%) and decreased to 78% at 7 days. Immunoreactivity for  $^{111}\text{In}$ -hu3S193 and  $^{125}\text{I}$ -hu3S193 at  $t = 0$  h, as determined by single-point binding assay, was 65 and 51.5%, respectively, and slowly decreased over time, not dropping markedly until 7 days after injection, at which time the %IR for  $^{111}\text{In}$ -hu3S193 was 27.5% and  $^{125}\text{I}$ -hu3S193 was 27%.

**Imaging.** Localization of  $^{111}\text{In}$ -hu3S193 in a single BALB/c mouse bearing an MCF-7 and control SW-1222 tumor over time, as determined by gamma camera imaging, is presented in Fig. 4. At 4 h, no tumor localization was evident, with the image showing generalized blood pool activity and slightly increased activity in the central portion of the scan corresponding to the cardiac area. At 24 h, minimal uptake was seen in the control tumor (left side of image), but there was definite localization of antibody to the MCF-7  $\text{Le}^y$ -expressing xenograft (right side of image). Over time with decreasing blood pool activity, the uptake in the MCF-7 tumor was more clearly defined. The mouse was sacrificed after the last image was obtained at 120 h. Radioactivity was clearly localized to the MCF-7 tumor, and the tumor:blood ratio was determined to be 6.07:1.

**Autoradiography and Immunohistochemistry.** The distribution of radioactivity via autoradiography, the location of viable tumor cells using hematoxylin staining, and antigen distribution as determined by immunoperoxidase techniques were compared in an MCF-7 xenograft removed at day 5 in the  $^{125}\text{I}/^{111}\text{In}$ -hu3S193 biodistribution study. Representative results are shown in Fig. 5. Hematoxylin staining indicated that the tumor contained viable tissue peripherally and a small amount in the center of the section, with a large area of central necrosis and connective tissue (Fig. 5B). Antigen ( $\text{Le}^y$ ) was distributed evenly throughout the section in areas corresponding to viable tumor cells (Fig. 5C). Control slides for antigen staining showed some

nonspecific staining in the connective tissue stroma but were negative in the tumor itself (Fig. 5D). Radioactivity, assessed by autoradiography, was distributed throughout regions of viable tumor including the central area of viable tumor cells, with little activity in the central necrotic area (Fig. 5A), indicating specific localization of radiolabeled hu3S193 to tumor cells. A similar even distribution of radioactivity throughout viable tumor cells was seen in all other time points studied (results not shown), and given differences in tumor sections, in particular the quantity of necrotic or connective tissue, there was no qualitative difference in distribution of radioisotope over time.

## DISCUSSION

The role of mAbs in the treatment of breast cancer is currently under active investigation, with a number of unmodified antibodies, radio-immunoconjugates, and antibody-chemotherapy conjugates being studied in the laboratory and in clinical trials. Among these is a humanized antibody directed against the p185<sup>HER2</sup> growth factor receptor (encoded by the *HER-2/neu* oncogene), which is overexpressed in 25–30% of all breast cancers (25). Phase II and Phase III studies of this antibody in patients with metastatic breast cancer showed an objective response rate of 12% (25), and higher response rates have been observed when combined with chemotherapy (26). This antibody has been recently approved by the Food and Drug Administration for use in patients with metastatic breast cancer overexpressing the HER-2 receptor.

In addition, a number of other  $\text{Le}^y$  antibodies have been developed and have reached different stages in preclinical evaluation and clinical testing. These include ABL 364 (BR55-2), an IgG3 antibody derived from the BR55-2 hybridoma (7). Murine ABL 364 administered to patients with cytokeratin-positive tumor cells in their marrow was

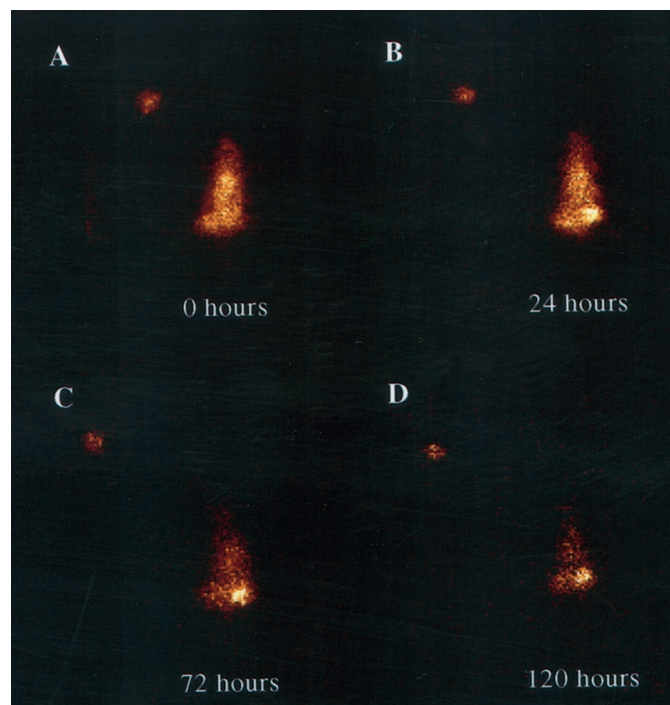


Fig. 4. Whole body scintigraphic images of radiolabeled  $^{111}\text{In}$ -CHX-A<sup>+</sup>-DTPA-hu3S193 in an athymic BALB/c nude mouse bearing s.c. MCF-7 (breast) tumor in the left flank (right side of image) and SW1222 colon tumor in the right flank (left side of image). Dorsal images were taken at 10 min (A), 24 h (B), 72 h (C), and 120 h (D) after injection of radiolabeled hu3S193, with the mouse supine on the gamma camera. A standard of known activity was included in the field of view and is visible in the upper left quadrant of each image.

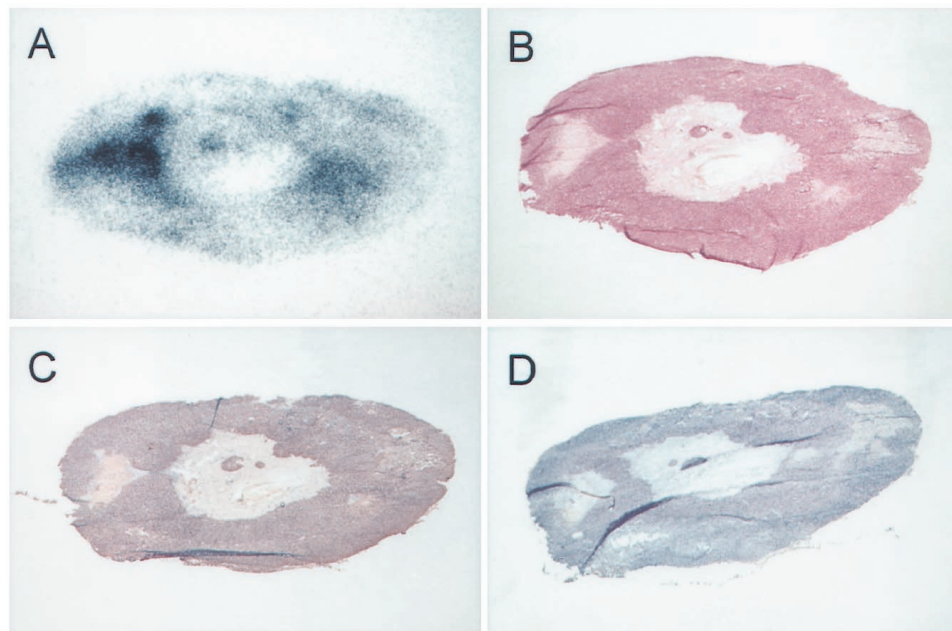


Fig. 5. Distribution of  $^{125}\text{I}/^{111}\text{In}$  radiolabeled hu3S193 in an MCF-7 tumor xenograft 120 h after antibody injection as determined by autoradiography (A). Localization of radiolabel is compared with the location of viable tumor cells by H&E staining (B) and to antigen distribution as shown by immunohistochemistry (C). D is a control slide for antigen detection in which huA33 was applied as the primary antibody instead of hu3S193, and negligible staining was noted.

shown to reduce or eliminate Le<sup>y</sup> antigen-cytokeratin (+) cells but not cytokeratin (+) cells in Le<sup>y</sup>-negative patients (27). However, a dose escalation study of murine BR55-2 in patients with metastatic breast cancer reported only minor clinical responses in 28.6% of patients, with HAMA limiting repeated cycles of treatment (28). A Phase I study with the LMB-1 immunotoxin, incorporating the murine anti-Le<sup>y</sup> monoclonal antibody B3 and recombinant *Pseudomonas* exotoxin, has also been performed in patients bearing solid epithelial tumors. Responses were observed in 5 of 38 patients studied; however, 90% of patients developed neutralizing antibodies against LMB-1 after one cycle of treatment (29).

Studies in nude mice bearing human lung carcinoma xenografts of another anti-Le<sup>y</sup> antibody, BR96, demonstrated that murine and chimeric BR96 were able to prevent or slow growth when administered soon after cell implantation but had only modest effects with staged tumors (22). In contrast, when chimeric BR96 was conjugated to doxorubicin, complete regressions of xenografted human lung, breast, and colon cancers grown s.c. in nude mice were seen (30). In Phase I and II clinical trials of chimeric BR96 (IgG1) conjugated to doxorubicin in patients with Le<sup>y</sup>-positive advanced stage carcinomas, limited response rates were observed, whereas gastrointestinal toxicity, which improved with implementation of steroid premedication, was demonstrated (31, 32).

We have examined the *in vivo* biodistribution and labeling stability of the recently humanized anti-Le<sup>y</sup> antibody 3S193, comparing  $^{125}\text{I}$ -,  $^{111}\text{In}$ -, and  $^{90}\text{Y}$ -labeled hu3S193 in an MCF-7 xenografted BALB/c nude mouse model. Excellent and specific tumor uptake was observed compared with a Le<sup>y</sup>-negative control tumor, with the peak tumor (MCF-7) uptake for all three isotopes occurring at 48 h. The %ID/g for both  $^{111}\text{In}$  and  $^{90}\text{Y}$  were significantly higher than  $^{125}\text{I}$ . In addition, both  $^{111}\text{In}$  and  $^{90}\text{Y}$  were retained within xenografts for a longer period of time than  $^{125}\text{I}$ . Lower absolute levels of iodine uptake compared with  $^{111}\text{In}$  in xenografts have been demonstrated in other studies (13), and this together with differences in tumor retention of radiolabel most likely represents differences in cellular processing of radiolabeled  $^{125}\text{I}$  as opposed to both  $^{111}\text{In}$  and  $^{90}\text{Y}$ . Catabolism of  $^{125}\text{I}$  linked to tyrosine results in the generation of [ $^{125}\text{I}$ ]mono-iodotyrosine within lysosomes, which rapidly leaves the cell via cell-mediated transport systems (18, 33, 34). In contrast, endocytosed  $^{111}\text{In}$ -DTPA-

antibodies are delivered to lysosomes and hydrolyzed by lysosomal enzymes into small molecular weight metabolites that are retained within tumor lysosomes (13, 33, 34).

Cellular processing of  $^{90}\text{Y}$  by tumor cells *in vitro* has been shown in other antibody-antigen systems to be similar to  $^{111}\text{In}$  (35) and is also reflected in similarities in distribution *in vivo* (36). It has been reported that although the pattern of uptake is comparable, superior tumor retention is obtained with the use of  $^{90}\text{Y}$  (36), a conclusion that this current study supports.

Within normal tissues, the uptake of  $^{111}\text{I}$  and  $^{90}\text{Y}$  in liver, spleen, and kidneys was higher than  $^{125}\text{I}$ . The higher uptake values in spleen and liver is consistent with known sequestration of radiometals in reticuloendothelial organs (36). This uptake in normal organs is not a consequence of specific targeting attributable to an absence of Le<sup>y</sup> antigen expression in these normal tissues of the mouse but is a reflection of blood flow and catabolism of the radiolabeled conjugates. The increased uptake of  $^{111}\text{In}$ - and  $^{90}\text{Y}$ -labeled antibody compared with  $^{125}\text{I}$  in the kidneys reflects differences in metabolism and excretion of radiometals (37). However, the increased renal uptake of  $^{90}\text{Y}$  compared with  $^{111}\text{In}$  may also reflect the conjugation of  $^{90}\text{Y}$ -CHX-A'-DTPA-hu3S193, given the observed low immunoreactivity of the labeling experiment presented, and warrants further investigation using chelating agents of enhanced stability for  $^{90}\text{Y}$  immunconjugates (37). The %ID/g of  $^{90}\text{Y}$  in the bone, assumed to represent bone marrow, was approximately double that of  $^{125}\text{I}$  and  $^{111}\text{In}$ ; however, the total amount present was negligible (2% ID/g), and differences were not statistically significant. Other studies have shown that accumulation of  $^{90}\text{Y}$  within bone is a concern with evidence that  $^{90}\text{Y}$  accumulates within the bone marrow (36) and indicates that  $^{111}\text{In}$  may underestimate  $^{90}\text{Y}$  bone marrow uptake.

The differences observed between isotopes in radiolabeling techniques and cellular processing were also reflected in the *in vivo* stability results. The percentage of  $^{125}\text{I}$ -bound radioactivity over time, as determined by ITLC, decreased rapidly, consistent with rapid release of free  $^{125}\text{I}$  from lysosomes. In contrast, only 2% of free  $^{111}\text{In}$  was detected over the same time period, again consistent with current literature suggesting retention of  $^{111}\text{In}$ -DTPA-lysine catabolites by tumor lysosomes (13, 33, 34). Retention of antigen binding for up to

5 days *in vivo* was also observed for both  $^{125}\text{I}$ - and  $^{111}\text{In}$ -labeled hu3S193.

Although promising, clinical responses with unconjugated mAbs in the therapy of solid tumors have been poorer and less consistent than with hematopoietic neoplasms (38–40), and there remains room for improvement. Given the high frequency of epithelial tumors expressing the Le<sup>y</sup> antigen and the high density of Le<sup>y</sup> on the surface of tumor cells, hu3S193 has potential therapeutic applications. The *in vivo* studies presented demonstrate that  $^{111}\text{In}$ - and  $^{90}\text{Y}$ -radiolabeled hu3S193 have favorable biodistribution characteristics, with high %ID/g uptake of both antibody bound isotopes within Le<sup>y</sup>-expressing MCF-7 breast xenografts. In contrast, the biological behavior of  $^{125}\text{I}$ -hu3S193, as demonstrated in this report, would indicate that  $^{131}\text{I}$  would not be the preferred isotope for this antibody-antigen system. Tumor localization of  $^{111}\text{In}$ -CHX-A"-DTPA hu3S193 was confirmed visually in imaging studies and by autoradiography, demonstrating good penetration of radionuclide to all areas of viable tumor cells. In addition to the direct targeting of the tumor by hu3S193, our previous studies have described the *in vitro* immune effector functions mediated by the IgG1 Fc portion of hu3S193 (8, 12). The antitumor effect of hu3S193 may be limited in the murine model used in the current study because of restricted murine serum complement activity. The potent *in vitro* antibody-dependent cellular cytotoxicity of hu3S193 would suggest that, in conjunction with potent complement-dependent cytotoxicity activity in the human, these humoral effects in a clinical setting would augment the therapeutic effects of targeted radiolabeled hu3S193.

hu3S193 has the theoretical advantage of reduced immunogenicity provided by humanization of an antibody, an assumption that has been supported by preliminary data with earlier, fully humanized antibodies (24, 41, 42), allowing multiple courses of treatment that have not been possible with murine or chimeric antibodies. The humanization of 3S193 has yielded a molecule with only 3–5% sequence homology to the parent murine antibody in the immunogenic variable domains. A similar humanization, through CDR grafting, to that of 3S193 has been described for an antihuman CD4 mAb using the same human framework (REI for variable light chain and KOL for variable heavy chain; Ref. 42). Preliminary clinical results in patients have been reported and show a lack of immunogenicity (42, 43).

The humanization strategy we adopted for hu3S193 and the results of clinical studies using mAbs with similar human frameworks provide evidence of the reduced potential for an immune response to hu3S193 in planned clinical trials.

Some Le<sup>y</sup> antigen expression was observed in the gastric glands of the stomach and basal intestinal glands of the small bowel of the BALB/c mice used in the current study, a similar distribution pattern to that reported previously in immunohistochemical studies of normal human tissues with other anti-Le<sup>y</sup> mAbs (6, 44). However, the current biodistribution study did not demonstrate increased specific targeting to the small bowel of the BALB/c mice (Fig. 2B). The expression of Le<sup>y</sup> antigen in normal human tissues (including the GI tract) is of concern in targeting strategies against this antigen; however, the accessibility of normal tissues to anti-Le<sup>y</sup> antibodies remains unclear. Results of studies with murine and chimeric antibodies against Le<sup>y</sup> suggest that gastric toxicity may be relevant in proposed clinical trials; however, significant toxicity has only been observed at protein doses >200 mg (31, 32). The optimal protein dose for effective targeting of Le<sup>y</sup> tumors (tumor:blood ratios, normal tissue uptake) is yet to be defined with carefully designed biodistribution and biopsy-based trials. In this context, high protein doses of anti-Le<sup>y</sup> antibodies reported to cause toxicities may not be required for effective tumor targeting.

The current model has demonstrated the stability of hu3S193, and

its characteristics and properties are well suited to beginning trials in the clinic.

## REFERENCES

- Smith, G., and Henderson, I. C. New treatments for breast cancer. *Semin. Oncol.*, 23: 506–528, 1996.
- De Vita, V. T., Hellman, S., and Rosenberg, S. A. Principles of chemotherapy. In: V. T. De Vita, Jr., S. Hellman, and S. A. Rosenberg (eds.), *Cancer: Principles and Practices of Oncology*, pp. 257–286, Philadelphia: J. B. Lippincott Co., 1985.
- Scott, A. M., and Cebon, J. Clinical promise of tumor immunology. *Lancet*, 349 (Suppl. II): 19–22, 1997.
- Hakomori, S. General concept of tumor-associated carbohydrate antigens: their chemical, physical and enzymatic basis. In: H. F. Oettgen, (ed.), *Gangliosides and Cancer*, pp. 93–102. Weinheim, Germany: VHC Publishers, 1989.
- Steplewski, Z., Blaszczyk-Thurin, M., Lubeck, M., Loibner, H., Scholz, D., and Koprowski, H. Oligosaccharide Y specific monoclonal antibody and its isotype switch variants. *Hybridoma*, 9: 201–210, 1990.
- Hellström, I., Garrigues, H. J., Garrigues, U., and Hellström, K. E. Highly tumor-reactive, internalizing, mouse monoclonal antibodies to Le<sup>y</sup>-related cell surface antigens. *Cancer Res.*, 50: 2183–2190, 1990.
- Steplewski, Z., Lubeck, M. D., Scholtz, D., Loibner, H., Smith, J. M., and Koprowski, H. Tumor cell lysis and tumor growth inhibition by the isotype variants of Mab BR55–2 directed against Y oligosaccharide. *In Vivo*, 5: 79–84, 1991.
- Kitamura, K., Stockert, E., Garin-Chesa P., Welt, S., Lloyd, K. O., Armour K. L., Wallace T. P., Harris, W. J., and Carr, F. J. Specificity analysis of blood group Lewis-y (Le<sup>y</sup>) antibodies generated against synthetic and natural Le<sup>y</sup> determinants. *Proc. Natl. Acad. Sci. USA*, 91: 12957–12961, 1994.
- Losman, M. J., DeJager, R. L., Monestier, M., Sharkey, R. M., and Goldenberg, D. M. Human immune response to anti-carcinoembryonic antigen murine monoclonal antibodies. *Cancer Res.*, 50 (Suppl.): 1055s–1058s, 1990.
- Liu, A. Y., Robinson R. R., Hellström, K. E., Murray, E. D., Jr., Chang, C. P., and Hellström, I. Chimeric mouse anti-human IgG1 antibody that can mediate lysis of cancer cells. *Proc. Natl. Acad. Sci. USA*, 84: 3439–3444, 1987.
- Jones, P. T., Dear, P. H., Foote, J., Neuberger, M. S., and Winter, G. Replacing the complementarity-determining regions in a human antibody with those from a mouse. *Nature (Lond.)*, 321: 522–524, 1986.
- Scott, A. M., Geleick, D., Rubira, M., Clarke, K., Nice, E. C., Smyth, F. E., Stockert, E., Richards, E., Carr, F. J., Harris, W. J., Armour, K. L., Rood, J., Kypridis, A., Kronina, V., Murphy, R., Lee, F.-T., Liu, Z., Kitamura, K., Ritter, G., Laughton, K., Hoffman, E., Burgess, A. W., and Old, L. J. Construction, production, and characterization of humanized anti-Lewis<sup>y</sup> monoclonal antibody 3s193 for targeted immunotherapy of solid tumors. *Cancer Res.*, 60: 3254–3261, 2000.
- King, D. J., Antoniwi, P., Owens, R. J., Adair, J. R., Haines, A. M. R., Farnsworth A. P. H., Finney, H., Lawson, A. D. G., Lyons, A., Baker, T. S., Baldock, D., Mackintosh, J., Gofton, C., Yarranton, G. T., McWilliams, W., Shochat, D., Lechner, P. H., Welt, S., Old, L. J., and Mountain, A. Preparation and preclinical evaluation of humanised A33 immunoconjugates for radioimmunotherapy. *Br. J. Cancer*, 72: 1364–1372, 1995.
- Levenson, A. S., and Jordan, V. C. MCF-7: the first hormone-responsive breast cancer cell line. *Cancer Res.*, 57: 3071–3078, 1997.
- Hunter, W. M., and Greenwood, F. C. Preparation of iodine-131 labeled growth hormone of high specific radioactivity. *Nature (Lond.)*, 194: 495, 1962.
- Wu, C., Kobayashi, H., Sun, B., Yoo, T. M., Paik, C. H., Gansow, O. A., Carrasquillo, J. A., Pastan, I., and Brechbiel, M. W. Stereochemical influence on the stability of radio-metal complexes *in vivo*. Synthesis and evaluation of the four stereoisomers of 2-(*p*-nitrobenzyl)-*trans*-CyDTPA. *Bioorg. Med. Chem.*, 5: 1925–1934, 1997.
- Nikula, T. K., Curcio, M. J., Brechbiel, M. W., Gansow, O. A., Finn, R. D., and Scheinberg, D. A. A rapid single vessel method for preparation of clinical grade ligand conjugated monoclonal antibodies. *Nucl. Med. Biol.*, 22: 387–390, 1995.
- Shih, L. B., Thorpe, S. R., Griffiths, G. L., Diril, H., Ong, G. L., Hansen, H. J., Goldenberg, D. M., and Mattes, M. J. The processing and fate of antibodies and their radiolabels bound to the surface of tumor cells *in vitro*: a comparison of nine radiolabels. *J. Nucl. Med.*, 35: 899–908, 1994.
- Lindmo, T., Boven, E., Cuttitta, F., Fedorko, J., and Bunn, P. A. Determination of the immunoreactive fraction of radiolabeled monoclonal antibodies by linear extrapolation to binding at infinite antigen excess. *J. Immunol. Methods*, 72: 77–89, 1984.
- Huseby, R. A., Maloney, T. M., and McGrath, C. M. Evidence for a direct growth-stimulating effect of estradiol on human MCF-7 cell *in vivo*. *Cancer Res.*, 44: 2654–2659, 1984.
- Osborne, C. K., Hobbs, K., and Clark, G. M. Effect of estrogens and antiestrogens on growth of human breast cancer cells in athymic nude mice. *Cancer Res.*, 45: 584–590, 1985.
- Scheiber, G., Hellstrom, K. E., and Hellstrom, I. An unmodified anticarcinoma antibody, BR96, localizes to and inhibits the outgrowth of human tumors in nude mice. *Cancer Res.*, 52: 3262–3266, 1992.
- Roberson, P. L., Buschbaum, D. J., Heidern, D. B., and Ten Haken, R. K. Three dimensional tumor dosimetry for radioimmunotherapy using serial autoradiography. *J. Radiat. Oncol. Biol. Phys.*, 24: 329–334, 1992.
- Co, M. S., Baker, J., Bednarik, K., Janzek, E., Neruda, W., Mayer, P., Plot, R., Stumper, B., Vasquez, M., Queen, C., and Loibner H. Humanised anti-Lewis Y antibodies: *in vitro* properties and pharmacokinetics in rhesus monkeys. *Cancer Res.*, 56: 1118–1121, 1996.
- Baselga, J., Tripathy, D., Mendelsohn, J., Baughman, S., Benz, C. C., Dantis, L., Sklarin, N. T., Seidman, A. S., Hudis, C. A., Moore, J., Rosen, P. P., Twaddell, T.,

- Henderson, I. C., and Norton, L. Phase II study of weekly intravenous recombinant humanised anti-p185<sup>HER2</sup> monoclonal antibody in patients with HER2/neu-overexpressing metastatic breast cancer. *J. Clin. Oncol.*, *14*: 737-744, 1996.
26. Pegram, M. D., Lipton, A., Hayes, D. F., Weber, B. L., Baselga, J. M., Tripathy, D., Baly, D., Baughman, S. A., Twaddell, T., Glaspy, J. A., and Slamon, D. J. Phase II study of receptor-enhanced chemosensitivity using recombinant humanized anti-p185HER2/neu monoclonal antibody plus cisplatin in patients with HER2/neu-overexpressing metastatic breast cancer refractory to chemotherapy treatment. *J. Clin. Oncol.*, *16*: 2659-2671, 1998.
  27. Schlimok, G., Pantel, K., Loibner, H., Fackler-Schwalbe, I., and Riethmuller, G. Reduction of metastatic carcinoma cells in bone marrow by intravenously administered monoclonal antibody: towards a novel surrogate test to monitor adjuvant therapies of solid tumors. *Eur. J. Cancer*, *31A*: 1799-1803, 1995.
  28. Theodoulou, M., Gilewski, T. A., Welt, S., Garin-Chesa, P., Stockert, E., Kitamura, K., Steplewski, Z., Koprowski, H., Norton, L., and Old, L. J. Anti-Lewis Y (Ley) monoclonal antibody (mAb) BR55-2 (IgG2a) in patients with advanced breast cancer. *Proc. Am. Soc. Clin. Oncol.*, *13*: 299, 1994.
  29. Pai, L. H., Wittes, R., Setser, A., Willingham, M. C., and Pastan, I. Treatment of advanced solid tumors with immunotoxin LMB-1: an antibody linked to *Pseudomonas* exotoxin. *Nat. Med.*, *2*: 350-353, 1996.
  30. Trail, P. A., Willner, D., Lasch, S. J., Henderson, A. J., Hofstead, S., Casazza, A. M., Firestone, R. A., Hellstrom, I., and Hellstrom, K. E. Cure of xenografted human carcinomas by BR96-doxorubicin immunoconjugates. *Science (Washington DC)*, *261*: 212-215, 1993.
  31. Sugarman, S., Murray J. L., Saleh, M., LoBuglio, A. F., Jones, D., Daniel, C., LeBherz, D., Brewer, H., Healey, D., Kelley, S., Hellstrom, K. E., and Onetto, N. A Phase I study of BR96-doxorubicin (BR96-DOX) in patients with advanced carcinoma expressing the Lewis Y antigen. *Proc. Am. Soc. Clin. Oncol.*, *14*: 473, 1995.
  32. Tolcher, A. W., Sugarman, S., Gelmon, K. A., Cohen, R., Saleh, M., Isaacs, C., Young, L., Healey, D., Onetto, N., and Slichenmyer, W. Randomized Phase II study of BR96-doxorubicin conjugate in patients with metastatic breast cancer. *J. Clin. Oncol.*, *17*: 478-484, 1999.
  33. Duncan, J. R., and Welch, M. J. Intracellular metabolism of indium-111-DTPA-labeled receptor targeted proteins. *J. Nucl. Med.*, *34*: 1728-1738, 1993.
  34. Press, O. W., Shan, D., Howell-Clark, J., Eary, J., Appelbaum, F. R., Matthews, D., King, D. J., Haines, A. M., Hamann, P., Hinman, L., Shochat, D., and Bernstein, I. D. Comparative metabolism and retention of iodine-125, yttrium-90 and indium-111 radioimmunoconjugates by cancer cells. *Cancer Res.*, *56*: 2123-2129, 1996.
  35. Duncan, J. R., Stephenson, M. T., Wu, H. P., and Anderson, C. J. Indium-111-diethylentriaminepentaacetic acid-octreotide is delivered *in vivo* to pancreatic, tumor cell, renal, and hepatocyte lysosomes. *Cancer Res.*, *57*: 659-671, 1997.
  36. Sharkey, R. M., Motta-Hennessy, C., Pawlyk, D., Siegel, J. A., and Goldenberg, D. Biodistribution and radiation dose estimates for yttrium- and iodine-labeled monoclonal antibody IgG and fragments in nude mice bearing human colonic tumor xenografts. *Cancer Res.*, *50*: 2330-2336, 1990.
  37. DeNardo, S. J., Zhong, G., Salako, Q., Li, M., DeNardo, G. L., and Meares, C. F. Pharmacokinetics of chimeric L6 conjugated to indium-111- and yttrium-90-DOTA-peptide in tumor-bearing mice. *J. Nucl. Med.*, *36*: 829-836, 1995.
  38. Goldenberg, D. M. Monoclonal antibodies in cancer detection and therapy. *Am. J. Med.*, *94*: 297-312, 1993.
  39. Janson, C. H., Tehrani, M., Wigzell, H., and Mellstedt, H. Rational use of biological response modifiers in hematological malignancies-a review of treatment with interferon, cytotoxic cells and antibodies. *Leuk. Res.*, *13*: 1039-1046, 1989.
  40. Sears, H. F., Atkinson, B., Mattis, J., Ernst, C., Herlyn, D., Steplewski, Z., Haysy, P., and Koprowski, H. Phase I clinical trial of monoclonal antibody in the treatment of gastrointestinal tumors. *Lancet*, *1*: 762-765, 1982.
  41. Caron, P. C., Co, M. S., Bull, M. K., Avdalovic, N. M., Queen, C., and Scheinberg, D. A. Biological and immunological features of humanized M195 (anti-CD33) monoclonal antibodies. *Cancer Res.*, *52*: 6761-6767, 1992.
  42. Pulito, V. L., Roberts, V. A., Adair, J. R., Rothermel, A. L., Collins, A. M., Varga, S. S., Martocello, C., Bodmer, M., Jolliffe, L. K., and Zivin, R. A. Humanization and molecular modeling of the anti-CD4 monoclonal antibody, OKT4A. *J. Immunol.*, *156*: 2840-2850, 1996.
  43. Delmonico, F. L., and Cosimi, A. B. Anti-CD4 monoclonal antibody therapy. *Clin. Transplant.*, *10*: 397-403, 1996.
  44. Pastan, I., Lovelace, E. T., Gallo, M. G., Rutherford, A. V., Magnani, J. L., and Willingham, M. C. Characterization of monoclonal antibodies B1 and B3 that react with mucinous adenocarcinomas. *Cancer Res.*, *51*: 3781-3787, 1991.